Proc. Natl. Acad. Sci. USA
Vol. 92, pp. 11200–11204, November 1995
Biochemistry

Effects of receptor dimerization on the interaction between the class I major histocompatibility complex-related Fc receptor and IgG

MALINI RAGHAVAN*, YONGPING WANG*†, AND PAMELA J. BJORKMAN‡§

*Division of Biology 156-29 and ‡Howard Hughes Medical Institute, California Institute of Technology, Pasadena, CA 91125

Communicated by Norman Davidson, California Institute of Technology, Pasadena, CA, July 28, 1995 (received for review June 1, 1995)

ABSTRACT **The neonatal Fc receptor (FcRn) transports maternal IgG from ingested milk in the gut to the bloodstream of newborn mammals. An FcRn dimer was observed in crystals of the receptor alone and of an FcRn–Fc complex, but its biological relevance was unknown. Here we use surface plasmon resonance-based biosensor assays to assess the role of FcRn dimerization in IgG binding. We find high-affinity IgG binding when FcRn is immobilized on a biosensor chip in an orientation facilitating dimerization but not when its orientation disrupts dimerization. This result supports a model in which IgG-induced dimerization of FcRn is relevant for signaling the cell to initiate endocytosis of the IgG–FcRn complex.**

Maternal IgG in milk is transported to the bloodstream of newborn rodents via the neonatal Fc receptor (FcRn) expressed in the gut (1). FcRn binds to the Fc portion of IgG at the pH of milk in the gut (pH 6.0–6.5). Upon binding, the FcRn–IgG complex is endocytosed and then transcytosed to the basolateral side of the cell, which faces the bloodstream. The slightly basic pH of blood (pH $\approx$ 7.5) causes IgG to dissociate from FcRn (2), thereby releasing maternal antibody in the bloodstream of the neonate and enabling the newborn to passively acquire immunity to antigens encountered by the mother. A human homolog mediates the transfer of maternal IgG across the placenta (3). FcRn resembles class I major histocompatibility complex (MHC) molecules (4, 5), which present peptide antigens to T cells (6). Both FcRn and class I molecules consist of a membrane-spanning heavy chain with three extracellular domains, α1, α2, and α3, that are noncovalently attached to a soluble light chain, β_2-microglobulin (β_2m) (7). The recently determined crystal structure of FcRn verified its structural similarity to class I MHC molecules and revealed an FcRn dimer of heterodimers (hereafter referred to as the FcRn dimer) mediated by contacts between the α3 and β_2m domains (8). The existence of the FcRn dimer on a membrane requires a "lying down" orientation of the receptors with their long axes nearly parallel to the plane of the membrane (Fig. 1*A*), by contrast to the "standing up" orientation generally assumed for class I MHC molecules, which are not observed to form dimers or other oligomers. Because of the 2:1 binding stoichiometry between FcRn and IgG (10), and because soluble FcRn is predominantly monomeric in solution (11), we previously suggested that the FcRn dimer could represent a receptor dimer induced by IgG binding (8) and assumed that the dimer could form in the absence of IgG in the FcRn crystals because of the high protein concentrations required for crystallization. The oligomeric state of the receptor on the membrane is unknown.

The same FcRn dimer was found in the low-resolution crystal structure of an FcRn–Fc complex (9), supporting the suggestion that FcRn dimers bind IgG on cell surfaces in a lying down orientation. However, the interpretation of the FcRn–Fc crystal structure is complicated by the packing in the cocrystals, which creates two distinct 2:1 complexes, only one of which incorporates the FcRn dimer. In the first 2:1 complex (the lying down complex; Fig. 1*A*), Fc contacts the FcRn dimer asymmetrically, so that most of the predicted contacts to Fc involve only one molecule of the FcRn dimer. An attractive feature of the lying down complex is that a signal for endocytosis of the FcRn–IgG complex could be binding of an IgG to one receptor, followed by recruitment of a second FcRn to form a receptor dimer in which the cytoplasmic domains are brought into spatial proximity. The second 2:1 complex (the standing up complex; Fig. 1*B*) does not involve the receptor dimer, and there is no contact between the two receptors upon binding Fc. Instead, Fc binds symmetrically between two FcRn molecules that are oriented with their long axes perpendicular to membrane. We previously used the results of mutagenesis studies (12) and steric considerations to argue that the 2:1 complex involving the FcRn dimer (the lying down complex) is relevant for binding of intact IgG at the cell surface (9). However, since most of the predicted FcRn contacts to Fc in the lying down complex involve only one molecule of the FcRn dimer (9), the contribution of the other FcRn molecule in the dimer to the overall affinity of the FcRn–IgG interaction was unclear. Here we used oriented coupling to a biosensor chip and a surface plasmon resonance (SPR) assay (13, 14) to investigate the relative affinities of FcRn molecules in which dimerization was facilitated and FcRn molecules in which dimerization was hindered. We present evidence that the FcRn dimer is required for high-affinity binding of IgG, thereby implying that FcRn dimerization is crucial for IgG binding at the cell surface and providing further support for existence of the lying down 2:1 FcRn–IgG complex. These results raise the possibility that FcRn may function like many other cell surface receptors in which ligand-induced dimerization is the primary event required for downstream signal transduction (15).

MATERIALS AND METHODS

Reagents. Iodoacetyl-LC-biotin (*N*-iodoacetyl-*N*-biotinylhexylenediamine) was obtained from Pierce. Rabbit anti-human β_2m and peroxidase-conjugated anti-rabbit antibodies for ELISAs were from Boehringer Mannheim. *N*-Ethyl-*N'*-(3-diethylaminopropyl)carbodiimide, *N*-hydroxysuccinimide, 2-(2-pyridinyldithio)ethaneamine, ethanolamine, BIAcore surfactant P20, certified CM5 sensor chips, and streptavidin-coated sensor chips were from Pharmacia Biosensor. Murine IgG1 was purchased from PharMingen.

The publication costs of this article were defrayed in part by page charge payment. This article must therefore be hereby marked "*advertisement*" in accordance with 18 U.S.C. §1734 solely to indicate this fact.

Abbreviations: β_2m, β_2-microglobulin; FcRn, Fc receptor, neonatal; MHC, major histocompatibility complex; RU, resonance units; SPR, surface plasmon resonance.

†Present address: Molecular Biophysics and Biochemistry, Yale University, New Haven, CT 06520.
§To whom reprint requests should be addressed.

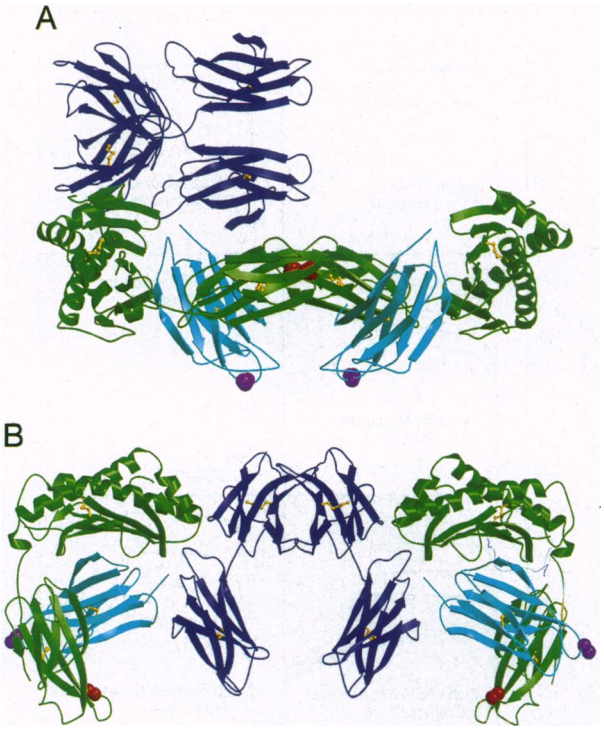

FIG. 1. Free thiols introduced into FcRn for oriented coupling highlighted on ribbon diagrams of the two different 2:1 FcRn–Fc complexes observed in cocrystals of FcRn and Fc (9). For cell surface FcRn, the membrane is assumed to be horizontal in each figure. The FcRn heavy chain is green, β_2m is light blue, Fc is dark blue, disulfide bonds are yellow, and introduced Cys residues are purple (FcRn D) and red (FcRn M). (*A*) Cys mutations highlighted on the lying down 2:1 complex of FcRn and Fc. Coupling of FcRn D (Cys introduced at β_2m residue 19; purple; 25–30 Å from the approximate center of the FcRn dimerization interface) to the biosensor chip is predicted to facilitate formation of the FcRn dimer, allowing formation of this 2:1 complex. Coupling of FcRn M (Cys introduced at the FcRn dimer interface at FcRn heavy chain residue 191; red) to the biosensor chip is predicted to hinder formation of the FcRn dimer, so that formation of this 2:1 complex would be impaired on the surface of the biosensor chip. (*B*) Cys mutations highlighted on the standing up 2:1 complex of FcRn and Fc that does not involve FcRn dimerization. If FcRn dimers are not involved in binding of IgG, there should be minimal or no effects of coupling via either of the introduced Cys residues.

Expression of Mutant FcRn Molecules. The cDNA encoding the truncated FcRn heavy chain was first altered by oligonucleotide-directed *in vitro* mutagenesis (16) to remove free sulfydryl groups that would interfere with coupling via introduced Cys residues (Cys-48 and Cys-226 were changed to Ser). For FcRn M, an additional mutation was introduced in the heavy chain gene to change Gly-191 to Cys. For FcRn D, a mutation was introduced into the cDNA encoding β_2m to change Lys-19 to Cys. After verifying the sequence of the altered cDNAs, the mutant heavy chain gene was subcloned into the expression vector pBJ5-GS (11), and the mutant light chain gene was subcloned into the expression vector pBJ1 (17). Cotransfection of FcRn and β_2m expression vectors into Chinese hamster ovary (CHO) cells and selection using the drug methionine sulfoximine were carried out as described (12). Cell supernatants were screened for protein expression by a sandwich ELISA, using the FcRn-specific monoclonal antibody 1G3 (12) as the capture antibody and a polyclonal antiserum against human β_2m to detect positive samples as described (18). Results were verified by immunoprecipitations with the 1G3 antibody. The highest expressing clones for FcRn D and M were grown in fifty 10-cm tissue culture plates, and the mutant proteins were purified from the supernatants by pH-dependent binding to a rat IgG column (11).

SPR-Based Biosensor Experiments. A BIAcore biosensor system (Pharmacia LKB Biotechnology) was used to measure FcRn–IgG binding interactions. This system includes a biosensor chip that has a gold surface coated with flexible dextran linkers to which biomolecules can be coupled. Binding interactions between the coupled molecules and a second molecule injected over the chip surface result in changes in the SPR signal that are read out in real time as resonance units (RU) (13, 14). RU values above 50 were considered significant. The derived data is in the form of sensorgrams (plots of RU versus time), which can be analyzed to estimate association and dissociation kinetics and binding constants. In the first set of experiments, IgG [M1/42, a rat IgG2a purified as described (12)] was immobilized to a biosensor chip surface using standard amine coupling chemistry (12), and different concentrations of FcRn D or M were injected over the IgG-coupled biosensor element. In the second set of experiments, FcRn D or M was immobilized using thiol chemistry as described below, and different concentrations of murine IgG1 were injected. In a third set of experiments, biotinylated FcRn D and M were immobilized on a streptavidin-coated sensor chip, and different concentrations of murine IgG1 were injected. Rat IgG2a was used in the first set of experiments rather than the murine IgG1 used in the second and third sets of experiments because the activity of murine IgG1 was found to be significantly affected by amine-based coupling. Flow rates of 5 μl/min were used for all of the experiments. Sensor chip surfaces were regenerated by injecting a pulse of 50 mM phosphate/150 mM NaCl, pH 7.5.

Thiol Coupling of FcRn to Biosensor Chips. FcRn M or D was incubated on ice for 3–4 hr with 20 mM cysteine HCl/20 mM $NaHCO_3$. Free cysteine was removed by two sequential centrifugations through Bio-Spin 30 chromatography columns (Bio-Rad) equilibrated in 10 mM citrate buffer (pH 4.0). The proteins were further diluted in the citrate buffer to a concentration of 25–50 μg/ml and immobilized by initial activation of the sensor chip with 0.05 M *N*-hydroxysuccinimide and 0.2 M *N*-ethyl-*N'*-(3-diethylaminopropyl)carbodiimide, followed by reaction with 80 mM 2-(2-pyridinyldithio)ethaneamine in 100 mM borate buffer (pH 8.5), and then injection of FcRn M or D. Excess reactive groups were deactivated by injecting 50 mM L-cysteine/1.0 M NaCl in 100 mM sodium formate buffer (pH 4.3).

Stoichiometry Measurements. Stoichiometries of FcRn–IgG complexes were calculated as described in the BIAcore methods manual. After immobilization of FcRn, the net SPR signals (the RU value 10–15 sec after the start of the dissociation phase) were recorded for IgG injections at concentrations between 15 and 20 μM. The equation

$$s = [RU_{(IgG)}/RU_{(FcRn)}] \times [\text{molecular weight}_{(FcRn)}/\text{molecular weight}_{(IgG)}]$$

was used to calculate s, the number of IgG molecules that bind per FcRn molecule.

Biotinylation of FcRn. FcRn D and FcRn M were biotinylated on the introduced Cys residue using iodoacetyl-LC-biotin. For this purpose, FcRn D or FcRn M protein in 50 mM Tris/5 mM EDTA, pH 8.3, was treated in the dark for 90 min with 0.9 molar equivalent of iodoacetyl-LC-biotin dissolved in dimethyl sulfoxide. The mixtures were subsequently chromatographed over a small gel-filtration column to remove excess biotin reagent.

Affinity Measurements of FcRn–IgG Complexes and Analysis of Dissociation Rates. High-affinity binding constants were calculated from estimates of the kinetic constants by nonlinear analysis of the association and dissociation curves using the BIAEVALUATION 2.0 software package. Binding constants (Table 1) were calculated assuming a single averaged

association rate constant and a single averaged dissociation rate constant. A detailed analysis of the dissociation curves (see below) shows the existence of high- and low-affinity populations; however, the high-affinity population predominates (>80%) over the concentration ranges used in these sets of experiments. The reported binding constants are therefore representative of the high-affinity population.

The dissociation phase of the sensorgrams was analyzed in detail for the binding of murine IgG1 to FcRn D or M immobilized directly via the respective thiol residues or via the biotin linker (Table 2). The BIAEVALUATON 2.0 software package was used to first fit the experimental dissociation curves to a single-exponential dissociation rate equation ($y = Re^{-k_d t}$, where k_d is the rate constant and R corresponds to the RU value at the start of the dissociation analysis). The experimental dissociation curves were next fit using a two-exponential dissociation rate equation [$y = R_{fast}\, e^{-k_{d(fast)}t} + R_{slow}\, e^{-k_{d(slow)}t}$, where $k_{d(slow)}$ and $k_{d(fast)}$ represent fast and slow rate constants, and R_{slow} and R_{fast} correspond to the fraction of complexes dissociating with each rate constant]. Using the BIAEVALUATION 2.0 software, an F test based comparison between derived χ^2 values for the single-exponential or two-exponential fits yielded an estimated probability that the second model is better than the first. In every case for which we report two k_d values, [$k_{d(slow)}$ and $k_{d(fast)}$; Table 2], the probability that the two-exponential dissociation model fit the experimental dissociation data better than a single-exponential model was in the range of 0.99–1.0.

RESULTS

The Effects of FcRn Orientation upon Affinity for IgG. Two mutant forms of soluble FcRn heterodimers [residues 1–269 of the rat FcRn heavy chain complexed with rat β_2m (11)] were generated to facilitate thiol coupling of FcRn on a biosensor chip in two defined orientations. Free sulfydryl residues were first removed from the FcRn heavy chain using site-directed mutagenesis (16) to change Cys-48 and Cys-226 to Ser residues. A Cys was then introduced at residue 19 of rat β_2m to make the FcRn D mutant (β_2m Lys19Cys) or at residue 191 of the FcRn heavy chain to make FcRn M (Gly191Cys). None of the residues that were changed in FcRn D or FcRn M are close to or at the predicted IgG binding interface deduced from the crystal structure of the FcRn–Fc complex (9); therefore, the modifications should not directly interfere with IgG binding (Fig. 1). Mutant proteins were purified from transfected cell supernatants by pH-dependent binding to a rat IgG column (11), thus verifying that the mutations did not significantly affect the interaction between FcRn and IgG. As further characterization of the mutants, IgG binding by both mutant receptors was characterized by coupling a rat IgG molecule on a biosensor chip and injecting either FcRn M or FcRn D proteins at pH 6.0 (Fig. 2 *A* and *B*). Comparisons of the derived affinities reveal only minor differences in IgG binding by either FcRn M or FcRn D (Table 1). Next, thiol chemistry was used to couple FcRn M or FcRn D to biosensor chips to evaluate the effects of FcRn orientation upon IgG binding. For these experiments, the FcRn molecules were coupled to a biosensor chip surface to a density of 2000–2200 RU, which should permit dimerization of the coupled receptors, since a coupling density of FcRn molecules of 2000 RU corresponds to 2.0 ng/mm^2 or two molecules per 10^4 Å^2 (100 Å × 100 Å). Coupling of FcRn D to a biosensor chip via the engineered Cys-19 of β_2m is predicted to promote the formation of the crystallographically observed FcRn dimer on the surface of the chip (Fig. 1*A*). Indeed, when high concentrations of IgG are injected (15–20 μM), we calculate a stoichiometry of 0.3–0.5 IgG per immobilized FcRn D (see *Materials and Methods*). Coupling of FcRn M via the introduced Cys at residue 191 of the FcRn heavy chain, which is located within the FcRn dimer

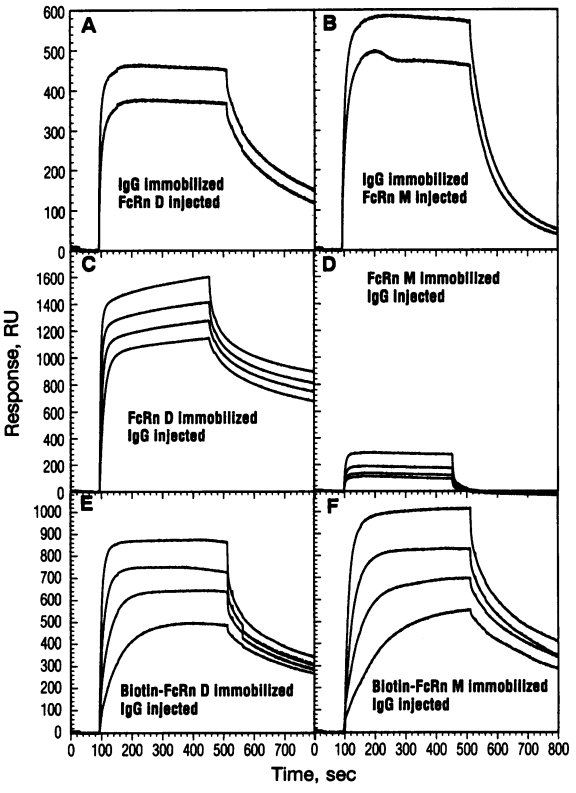

FIG. 2. SPR assays of the interaction between FcRn D or FcRn M with IgG. Observed RU are plotted as a function of time (sensorgrams) in each panel. Sensor chip surfaces were regenerated between different injections by injecting a pulse of 50 mM phosphate/150 mM NaCl, pH 7.5. (*A* and *B*) FcRn D or FcRn M samples were injected over rat IgG2a immobilized on a biosensor chip to a final response of 1640 RU (1.6 ng/mm^2) using amine coupling chemistry. Two injections corresponding to 1 μM and 2 μM FcRn D (*A*) and FcRn M (*B*) were performed. (*C* and *D*) FcRn D and FcRn M were immobilized on different flow cells of the same biosensor chip using thiol coupling chemistry. Four different concentrations of murine IgG1 (530 nM to 4.3 μM) were injected over FcRn D coupled to a density of 2200 RU (2.2 ng/mm^2) (*C*) or FcRn M coupled to a density of 2000 RU (2.0 ng/mm^2) (*D*) or over a blank flow cell (data not shown). For FcRn M, a net positive SPR signal >50 RU is seen only when the concentration of injected IgG is >4 μM. (*E* and *F*) Biotinylated FcRn D and FcRn M were injected over different flow cells of a commercially available streptavidin-coated sensor chip. Four different concentrations of murine IgG1 (375 nM to 3 μM) were injected over FcRn D coupled to a density of 1200 RU (1.2 ng/mm^2) (*E*) or FcRn M coupled to a density of 1750 RU (1.75 ng/mm^2) (*F*).

interface (Fig. 1*A*) (8), should disrupt formation of the FcRn dimer because the molecules would be tethered at their dimerization site to the dextran matrix of the biosensor chip. IgG binding by immobilized FcRn M is markedly impaired compared to FcRn D (Table 1 and Fig. 2 *C* and *D*). It is not possible to estimate a stoichiometry for the FcRn M–IgG interaction, since very high IgG concentrations would be required to observe saturation. Fig. 2 *C* and *D* compares the binding at pH 6.0 of different concentrations of a murine IgG injected over immobilized FcRn D or immobilized FcRn M. The estimated affinity of FcRn M for IgG is at least 100-fold lower than the affinity of FcRn D for IgG (Table 1). Because only small affinity differences were observed between the two forms of FcRn when binding to immobilized IgG (Fig. 2 *A* and *B*; Table 1), these results suggest that the marked impairment of IgG binding when FcRn M is coupled to the chip is a direct consequence of its orientation on the chip surface rather than an effect of the introduced mutations.

Impaired IgG binding by immobilized FcRn M can be prevented by incorporating a long linker arm between thiol

Table 1. Effects of FcRn orientation upon affinity for IgG: Comparison of the affinities of FcRn M–IgG and FcRn D–IgG complexes

Experiment	K_d, nM		Ratio of K_d values FcRn M/ FcRn D
	FcRn M	FcRn D	
IgG immobilized	240.0 ± 50.3	80.2 ± 26.7	3.0
FcRn immobilized by direct thiol coupling	>4000	22.0 ± 4.5	>100
FcRn immobilized via biotin linker	189.0 ± 34.9	103.5 ± 11.1	1.8

For the IgG immobilized experiments, a rat monoclonal IgG2a antibody was immobilized to a final response of 1640 RU, and FcRn D or FcRn M was injected. For FcRn immobilized by direct thiol coupling, mutant FcRn molecules were coupled via introduced Cys residues to densities of 2200 RU (FcRn D) and 2000 RU (FcRn M) and a murine IgG1 was injected. For FcRn immobilized via biotin linker, FcRn M or FcRn D was coupled ≈20 Å from the biosensor surface to densities of 1750 and 1200 RU, respectively, and murine IgG1 was injected. Under conditions where FcRn M is directly coupled to the chip surface, there is no specific binding observed at IgG concentrations below 4 μM, suggesting a micromolar (or weaker) affinity constant for the interaction. The absolute values of the high-affinity K_d values determined for FcRn D under the three different experimental conditions vary 4- to 5-fold, representing the level of experimental error introduced by different coupling methods or the use of different chips and/or varying affinities of FcRn for different IgGs.

residue 191 and the surface of the biosensor chip. If the free thiol groups on FcRn D or M are derivatized with iodoacetyl-LC-biotin and subsequently coupled to avidin immobilized on a biosensor chip, thus allowing more than a 20 Å spacer between the respective thiol groups and the surface of the chip, the affinities and dissociation rate properties for IgG binding by FcRn M and FcRn D are very similar (Fig. 2 *E* and *F*; Tables 1 and 2). In addition, the calculated stoichiometry of the FcRn–IgG interaction is 0.5 IgG per FcRn M or FcRn D immobilized via the biotin linker. These results suggest that FcRn can form dimers when a narrow linker group is attached to cysteine residues at the dimerization interface, provided there is sufficient room above the surface of the biosensor chip to allow the two molecules to come together. When tethered directly to the chip, as in the experiment depicted in Fig. 2*D*, the dimerization interface is expected to be much less accessible.

Comparison of Observed Dissociation Rate Constants (k_d) and Net SPR Signals (R_t) of FcRn D–IgG and FcRn M–IgG Complexes as a Function of IgG Concentration and FcRn Coupling Density. Biphasic binding curves have previously been observed for the interaction of IgG with FcRn in brush border membrane extracts from neonatal rats, suggesting the existence of two populations of FcRn with differing affinities for IgG (19). Consistent with this observation, we find that the assumption of two populations of complexes with fast and slow dissociation rate constants (see *Materials and Methods* and Table 2) approximates the BIAcore experimental data better than the assumption of a single homogeneously dissociating population. The hypothesis that the slow dissociating species corresponds to a high-affinity 2:1 FcRn–IgG complex and the fast dissociating species corresponds to a low-affinity 1:1 FcRn–IgG complex is supported by the following trends deduced from the data in Table 2. (*i*) For a given coupling density of FcRn on the surface of the chip, the fast dissociating species becomes more predominant at high IgG concentrations, which are expected to drive the formation of 1:1 FcRn–IgG complexes. (*ii*) For a given IgG concentration, as the coupling density of FcRn is increased (facilitating FcRn dimerization), the slow dissociating species becomes more predominant.

With the assumption that the slow dissociating species corresponds to a high-affinity 2:1 FcRn–IgG complex and the fast dissociating species corresponds to a lower affinity 1:1 FcRn–IgG complex, the data presented in Table 2 demonstrate the impairment of dimerization of immobilized FcRn M compared to FcRn D. For example, when a low density (2000–2900 RU) of FcRn M molecules is coupled to the chip,

Table 2. Comparison of observed rate constants (k_d) and net SPR signals (R_t) of FcRn D–IgG and FcRn M–IgG complexes as a function of IgG concentration and FcRn coupling density

Coupled molecule	Coupling density, RU	$k_{d(slow)}$ × 10^3, s^{-1}	$k_{d(fast)}$ × 10^3, s^{-1}	IgG, μM	R_t, RU	% slow	% fast
FcRn D	2200	1.7 ± 0.3	24 ± 7	0.13	860	88.6	11.4
				17.17	1480	83.0	17.0
FcRn M	2000	—	31 ± 3	4.29	60	0	100
				17.17	110	0	100
FcRn M	2900	3.8 ± 0.4	39 ± 6	0.58	70	44.6	55.4
				18.67	200	38.6	61.4
FcRn D	5400	1.9 ± 0.3	43 ± 16	0.15	1060	100	0
				9.33	2320	88.3	11.7
FcRn M	6600	2.8 ± 0.4	29 ± 10	0.15	380	87.3	12.7
				9.33	1120	78.7	21.3
Biotin M	1750	1.6 ± 0.2	18 ± 2	0.38	513	89.7	10.3
				3.00	817	71.8	28.2
Biotin D	1200	1.7 ± 0.8	27 ± 3	0.38	439	92.4	7.6
				3.00	641	84.0	16.0

FcRn M and FcRn D were coupled via their introduced Cys residues to the specified densities using a direct thiol coupling protocol or via a biotin linker (biotin D and biotin M). Various concentrations of murine IgG1 were injected within the specified concentration ranges. In order to disregard contributions to the SPR signal from buffer differences and nonspecific binding, the net signal observed is presented at each concentration of injected IgG as R_t, the RU value 10–15 sec after the start of the dissociation phase. R_t values above 50 RU were considered significant. $k_{d(slow)}$ and $k_{d(fast)}$ represent derived fast and slow rate constants (see *Materials and Methods*) and % slow and % fast correspond to R_{slow} and R_{fast} (the fraction of R_t dissociating with the two respective rate constants). The fast and slow rate constants are presumed to correspond to 1:1 (low affinity) and 2:1 (high affinity) FcRn–IgG complexes, respectively (see text). When FcRn M is coupled to the chip at low densities (2000–3000 RU), most of the FcRn M–IgG complexes show fast dissociation rates (a low-affinity interaction), and high IgG concentrations are required to observe significant R_t values, illustrating impaired IgG binding by FcRn M.

either none of the FcRn M–IgG complexes or only a minority population show the slow dissociation rate, and high IgG concentrations are required to observe a net positive SPR signal (R_t). By contrast, at a similar coupling density, the majority of FcRn D molecules form high-affinity complexes with IgG that show the slow dissociation rate, and the net SPR signal is large. When a high density (6600 RU) of FcRn M molecules is coupled to the chip, high-affinity binding of FcRn M is not completely inhibited. However, only a fraction of the total FcRn M molecules are able to bind with high affinity, as suggested by the significantly lower net SPR signals obtained for FcRn M compared to FcRn D.

DISCUSSION

When a low density of FcRn M is coupled to the chip, no net equilibrium responses are observed when IgG is injected at concentrations below 4 μM, suggesting that the affinity constant for IgG binding under conditions where FcRn dimerization is nearly completely prevented is micromolar or weaker. In contrast, for FcRn D–IgG complexes, the high-affinity binding constant is 22.0 ± 4.5 nM (Table 1 and Fig. 2*C*). This binding constant is consistent with previous estimates derived from analyses of IgG binding to cell surface FcRn (12, 19), which implies that FcRn dimerizes at the cell surface when IgG is bound. The affinity loss from impaired dimerization is thus estimated to be >100-fold. A comparable loss in affinity between FcRn and IgG occurs as the pH is raised from 6.0 to 7.0 (22). The question therefore arises of whether the formation and disruption of the FcRn dimer could account for the sharply pH-dependent interaction with IgG. Imidazole side chains of histidine residues usually deprotonate over the pH range of 6.0–7.0; therefore, histidine residues at the FcRn dimer interface could bring about a pH-dependent destabilization of the dimer by the neutralization of positive charges above the pK_a values of the histidine residues. Two histidine residues are located at the FcRn dimer interface: residues 250 and 251 in the α3 domain of the FcRn heavy chain. Previous mutagenesis studies of the histidine pair showed that alteration of these residues resulted in a mutant FcRn molecule with ≈6-fold reduced affinity for IgG (12). Because these residues do not contact Fc directly (9), their effect on the affinity of FcRn for IgG must be due to participation in FcRn dimer formation. Titration of one or both residues of the histidine pair in wild-type FcRn could indirectly affect its affinity for IgG by stabilizing the FcRn dimer at pH 6.0–6.5 (permissive for IgG binding) and destabilizing the FcRn dimer at pH values above 7.0–7.5 (nonpermissive for IgG binding), thereby providing a mechanism to partially account for the pH-dependent alteration of the FcRn–IgG affinity. Other mechanisms such as titration of histidine residues at the IgG–FcRn interface must also contribute to the overall affinity transition, since the histidine pair mutant binds IgG in a pH-dependent manner (12).

In summary, we have demonstrated that the binding of IgG to FcRn is strongly influenced by the orientation of FcRn on the surface of a biosensor chip. The methods described here should be generally applicable to assess the importance of receptor oligomerization for the many other receptors that dimerize in response to ligand binding and for investigating the functional significance of higher order structures sometimes observed in crystallographic analyses—e.g., the crystallographically observed dimer of class II MHC molecules (20). Similar methods have been used to study a 1:1 human growth hormone–hormone receptor complex, a complex that normally shows 2:1 receptor to hormone stoichiometry due to hormone-induced receptor dimerization (21). The results presented here provide strong evidence that the crystallographically observed FcRn dimer of heterodimers is necessary for high-affinity IgG binding and directly support the existence of the lying down 2:1 FcRn–IgG complex (Fig. 1*A*) at the cell surface. The formation of both lying down and standing up complexes is possible in the event that two adjacent membranes are sufficiently close to allow formation of networks of FcRn–IgG complexes consisting of lying down FcRn dimers bridged by IgG (9). Parallel adjacent membranes exist in the microvilli of brush borders of intestinal epithelial cells, where FcRn is expressed and functions (1). Thus, although the data presented in this paper strongly support the hypothesis that FcRn dimerization is required for high-affinity binding of IgG, the interactions that form the standing up 2:1 complex may have some physiological relevance.

A K_d in the micromolar range for the dimerization-impaired FcRn, compared to a nanomolar K_d for dimerization-competent FcRn, is surprising in light of the crystal structure of the FcRn–Fc complex (9), which shows only a few contacts between Fc and the second molecule of the FcRn dimer. However, FcRn dimerization could alter its conformation so as to enhance the IgG binding affinity. If dimeric FcRn molecules do not preexist at the cell surface but are induced by IgG binding, FcRn dimerization could serve as a signal for the initiation of endocytosis of FcRn–IgG complexes, by analogy to activation of many growth factor and cytokine receptors by ligand-induced dimerization (15).

We thank D. Vaughn, W. P. Burmeister, and J. Harber for critical review of the manuscript and A. Chirino for help in making Fig. 1. This work was supported by the Howard Hughes Medical Institute (P.J.B.), a postdoctoral fellowship from the Cancer Research Institute (M.R.), and a Caltech Summer Undergraduate Research Fellowship (Y.W.).

1. Rodewald, R. (1973) *J. Cell Biol.* **58,** 189–211.
2. Rodewald, R. & Kraehenbuhl, J.-P. (1984) *J. Cell Biol.* **99,** 159s–164s.
3. Story, C. M., Mikulska, J. E. & Simister, N. E. (1994) *J. Exp. Med.* **180,** 2377–2381.
4. Simister, N. E. & Mostov, K. E. (1989) *Nature (London)* **337,** 184–187.
5. Simister, N. E. & Mostov, K. E. (1989) *Cold Spring Harbor Symp. Quant. Biol.* **54,** 571–580.
6. Townsend, A. & Bodmer, H. (1989) *Annu. Rev. Immunol.* **7,** 601–624.
7. Simister, N. E. & Rees, A. R. (1985) *Eur. J. Immunol.* **15,** 733–738.
8. Burmeister, W. P., Gastinel, L. N., Simister, N. E., Blum, M. L. & Bjorkman, P. J. (1994) *Nature (London)* **372,** 336–343.
9. Burmeister, W. P., Huber, A. H. & Bjorkman, P. J. (1994) *Nature (London)* **372,** 379–383.
10. Huber, A. H., Kelley, R. F., Gastinel, L. N. & Bjorkman, P. J. (1993) *J. Mol. Biol.* **230,** 1077–1083.
11. Gastinel, L. N., Simister, N. E. & Bjorkman, P. J. (1992) *Proc. Natl. Acad. Sci. USA* **89,** 638–642.
12. Raghavan, M., Chen, M. Y., Gastinel, L. N. & Bjorkman, P. J. (1994) *Immunity* **1,** 303–315.
13. Malmqvist, M. (1993) *Nature (London)* **361,** 186–187.
14. Fägerstam, L. G., Frostell-Karlsson, A., Karlsson, R., Persson, B. & Rönnber, I. (1992) *J. Chromatogr.* **597,** 397–410.
15. Heldin, C.-H. (1995) *Cell* **80,** 213–223.
16. Kunkel, T. A., Roberts, J. D. & Zakour, R. A. (1987) *Methods Enzymol.* **154,** 367–382.
17. Lin, A. Y., Devaux, B., Green, A., Sagerström, C., Elliott, J. F. & Davis, M. M. (1990) *Science* **249,** 677–679.
18. Fahnestock, M. L., Tamir, I., Narhi, L. & Bjorkman, P. J. (1992) *Science* **258,** 1658–1662.
19. Wallace, K. H. & Rees, A. R. (1980) *Biochem. J.* **188,** 9–16.
20. Brown, J. H., Jardetzky, T. S., Gorga, J. C., Stern, L. J., Urban, R. G., Strominger, J. L. & Wiley, D. C. (1993) *Nature (London)* **364,** 33–39.
21. Cunningham, B. C. & Wells, J. A. (1993) *J. Mol. Biol.* **234,** 554–563.
22. Raghavan, M., Bonagura, V. R., Morrison, S. L. & Bjorkman, P. J. (1995) *Biochemistry*, in press.